SCHEDULING THE CHARGE OF ELECTRIC VEHICLES INCLUDING REACTIVE POWER SUPPORT: APPLICATION TO A MEDIUM-VOLTAGE GRID

Biswarup Mukherjee[*], *Georges Kariniotakis, Fabrizio Sossan*

MINES ParisTech - PSL University, Centre PERSEE
Sophia Antipolis, France
* biswarup.mukherjee@mines-paristech.fr

Keywords: Electric Vehicles, Smart charging, Distribution grids, Smart grids, Optimal power flow

Abstract

The simultaneous charging process of multiple electric vehicles (EVs) may cause violations of power distribution grids' operational constraints, such as voltage levels outside statutory limits, line currents above lines' ampacities, and congestion at the substation transformer. This paper investigates the impact on a medium voltage distribution grid of i) uncoordinated charging, ii) coordinated grid-aware charging, and iii) coordinated grid-aware charging of EVs with reactive power support for voltage regulation. In all these cases, the EVs' charging policy is determined with an optimal power flow (OPF) problem, where suitable sets of constraints are modeled to reproduce each specific case. Results are investigated for the 14-bus CIGRE MV benchmark network. The proposed methods are useful for grid operators to identify suitable control strategies for EV charging.

1 Introduction

In 2017, 27% of the total greenhouse gas emissions in EU-28 are due to the transport sector [1]. In this context, electric vehicles (EVs) play a crucial role in decarbonizing road transport. With the increasing trend in the number of EV owners, the EV charging demand is also increasing, impacting the power sector. Simultaneously charging a large number of EVs determine a substantial increase of the peak demand in distribution grids and may cause substation power transformers' overloads, line currents above the cable ampacities, and voltage levels outside the allowed margins, requiring distribution system operators (DSOs) to undertake expensive grid reinforcements (e.g., [2]). In order to alleviate the impact of uncoordinated charging of many EVs, smart charging of EVs has widely been proposed in the existing literature to distribute the charging demand of EVs over a longer time horizon, achieving effective congestion management (e.g., [3, 4]).

This paper investigates the impact of different charging strategies for EVs on medium-voltage (MV) distribution grids and on recharging times performance. Three charging strategies are considered: uncoordinated charging (where each EV seeks to minimize its own recharging time, regardless of grid condition and others), grid-aware coordinated charging (where EVs are charged considering the constraints of the distribution grid), and grid-aware coordinated charging with reactive power support, where the spare capacity of the chargers is controlled to provide voltage regulation to the MV grid. The charging strategies are formulated by leveraging an optimal power flow (OPF) problem with linearized grid models from the literature

[4]. The OPF has a common baseline structure, where the constraints are adapted to represent the three strategies described above. This stands as the main contribution of this paper.

The paper is organized as follows. Section 2 states the problem and introduces the models. The OPF model for the recharging strategies is described in Section 3. Section 4 describes the case study. Results are presented and discussed in Section 5. Finally, Section 6 summarizes conclusions.

2 Problem statement and models

2.1 Problem statement

We consider a power distribution grid (such as the one in Fig. 1) interfacing loads (e.g., commercial and residential), possibly distributed generation, and EVs chargers. Distribution grids are designed to host prescribed levels of power demand. Larger demand levels might determine violations of their operational requirements. Operational requirements that distribution grid operators (DSOs) need to ensure are voltage levels inside statutory limits, line currents below cable ampacities, and power flow at the substation within the transformer rating. This paper investigates how these constraints can be embedded and enforced in the decision-making problem of EVs' charging.

2.2 Power grid model

The nodes of the network are referred with the index $n = 1, \ldots, N$, where N is the total number of nodes. The index
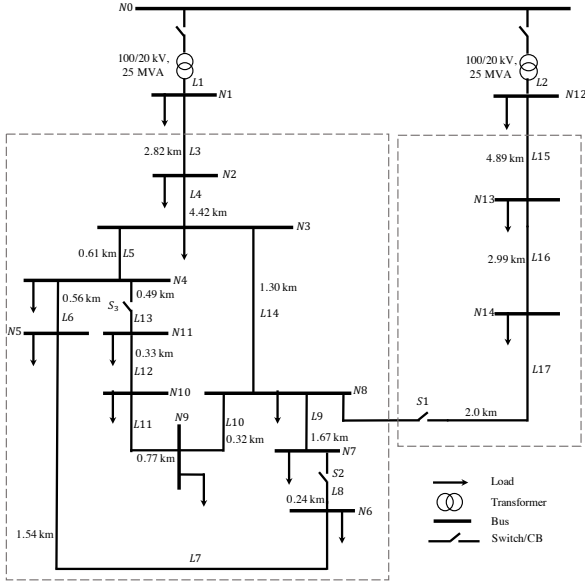
Fig. 1 Topology of the CIGRE European MV distribution network benchmark for residential system [5].

$t = 1, \ldots, T$ refers to the time interval, where T is the total number of samples. The time horizon $1, \ldots, T$ refers to the recharging horizon for the EVs. In the rest of this paper, we will refer to overnight charging, although the formulation is general and can be applied to other cases. Time dynamics need to be considered to model both time-variant power demand, and because the EVs' charging process is inherently time dependant due to the state-of-charge constraints of the EVs. The active and reactive power nodal injections at node n and time interval t is:

$$P_{tn} = P_{tn}^{(net)} + P_{tn}^{(EV\ nodal)} \tag{1a}$$

$$Q_{tn} = Q_{tn}^{(net)} + Q_{tn}^{(EV\ nodal)} \tag{1b}$$

for all nodes of the grid, where $P_{tn}^{(net)}$ is the net demand (i.e., power demand minus local renewable generation) and $P_{tn}^{(EV\ nodal)}$ is the total power demand of EVs. The former is an input of the problem, whereas the latter depends on the charging policy and is computed as described next.

Voltage levels at the nodes of the grid and the current values in the lines (voltage magnitudes, and line current magnitudes) depend on the grid topology, cables' parameters, voltage at the slack node, and nodal injections. They are modelled with load flow equations, that we generically denote in the following with functions f_n for the voltage magnitude and h_l for line current magnitudes:

$$v_{tn} = f_n \left(P_{t1}, \ldots, P_{tN}, Q_{t1}, \ldots, Q_{tN}, v_0, Y \right) \tag{2}$$

$$i_{tl} = h_l \left(P_{t1}, \ldots, P_{tN}, Q_{t1}, \ldots, Q_{tN}, v_0, Y \right), \tag{3}$$

where Y is the admittance matrix of the grid (built using the grid topology information and cable parameters), and v_0 is the voltage at the slack bus.

Load flow equations are nonlinear and their inclusion in optimization problems determines nonconvex formulations. To increase tractability, we linearize (2) and (3) using the method proposed in [6] based on sensitivity coefficients, whose performance has been investigated in [7], and as done in [8].

2.3 Modelling the charging of EVs

Let $v = 1, \ldots, V$ denote the index of a vehicle, where V is the total number of vehicles. The charging power of a vehicle v is limited by the rated power of the converter, denoted by $\overline{S}_v^{(EV)}$ (in kVA). Assuming the capability of the charger is independent from the voltage of the AC grid and of the DC bus, the apparent power limit of the charger is (for all t and v):

$$\left(P_{tv}^{(EV)} \right)^2 + \left(Q_{tv}^{(EV)} \right)^2 \leq \left(\overline{S}_v^{(EV)} \right)^2 \tag{4a}$$

$$P_{tv}^{(EV)} \geq 0 \tag{4b}$$

where $Q_{tv}^{(EV)}$ is the reactive power of the charger. Eq. (4b) reflects the fact that the vehicle can charge only, as opposed to vehicle-to-grid (V2G, implemented by bidirectional chargers), where EVs can possibly discharge to support the grid. Eq. (4) characterizes the "capability curve" of controlled rectifiers implemented in EV chargers. In this case, the capability curve extends to 2 quadrants of the P-Q plane, corresponding to non-negative active power and positive/negative reactive power.

The EV charging process is modelled accounting for the state-of-charge (SOC) of the vehicle. The index $v = 1, \ldots, V$ denotes the index of the EVs, where V is the total number of vehicles. The SOC of vehicle v is modelled by propagating a initial state-of-charge value, SOC_{0v}, and as a function of the non-negative charging power $P_{tv}^{(EV)}$ (in kW) and charging efficiency η. Self-discharge is not modelled as for li-ion batteries is typically small. The SOC model is:

$$\mathrm{SOC}_{tv} = \mathrm{SOC}_{t-1v} + \eta \frac{T_S}{E_v} P_{tv}^{(EV)}, \qquad P_{tv}^{(EV)} \geq 0 \tag{5}$$

for $t = 1, \ldots, T$, where T_s is the sampling time (in hours), and E_v is the nominal energy capacity of the EV's battery (kWh).

The link between the nodal injections of EVs, $P_{tn}^{(EV\ nodal)}$, $Q_{tn}^{(EV\ nodal)}$ in (1), and the charging of the single vehicles $P_{tv}^{(EV)}$ is given by the locations where the EVs charge. The charging location of EV v is encoded in the sequence of binary variables $b_{1v}, b_{2v}, \ldots, b_{Nv}$, that contains one 1 in the node where the EV charges, and N-1 0's at all other nodes.

Ultimately, the nodal EV injections are given by:

$$P_{tn}^{(EV\ nodal)} = \sum_{v=1}^{V} b_{nv} P_{tv}^{(EV)} \tag{6}$$

for all n. The matrix of $N \times V$ binary variables b_{nv} can be interpreted as the map reporting the recharging spots of all EVs. It is an input to the problem.

3 Methods

Three charging policies of EVs are considered: uncoordinated charging of multiple EVs, grid-aware coordinated charging, and grid-aware coordinated charging with reactive power support from the chargers. Their formulations are described next. For exemplifying the context, we consider a scenario where the EVs recharge overnight to achieve a target SOC level (e.g., a full recharge) necessary to meet the driving demand starting from an initial SOC value. The initial SOC is given by the state at which the EVs arrive at their parking (and charging) location. Both the initial SOC level and the target SOC level are inputs to the problem. They are respectively denoted by SOC_{0v} and $\text{SOC}_v^\star$. The main step and input data required for the formulation are illustrated in Fig. 2.

3.1 Uncoordinated charging

All EVs charge with the sole objective of minimizing the respective recharging time, independently from the state of the grid and of other EVs. Based on this requirement, we can then formulate a decision-making problem where the EVs' charging power is such that all vehicles reach as quick as possible the respective target state-of-charge level, $\text{SOC}_v^\star$. In this case, the chargers, modelled with (4), supply only active power since, not only reactive power is not conducive to recharge the vehicles, but it would also limit the capability of the charger. The decision-making problem is:

$$\underset{P_{11}^{(\text{EV})},\dots,P_{TV}^{(\text{EV})}\in\mathbb{R}_+}{\arg\min}\left\{\sum_{t=1}^{T}\sum_{v=1}^{V}\left(\text{SOC}_{tv}-\text{SOC}_v^*\right)^2\right\} \quad (7a)$$

subject to

$$\text{SOC}_{tv}=\text{SOC}_{t-1v}+\eta\frac{T_S}{E_v}P_{tv}^{(\text{EV})} \qquad \text{for all } t \text{ and } v \quad (7b)$$

$$0\leq\text{SOC}_{tv}\leq 100\%, \qquad \text{for all } t \text{ and } v \quad (7c)$$

$$0\leq P_{tv}^{(\text{EV})}\leq\overline{S}_v^{(\text{EV})} \qquad \text{for all } t \text{ and } v \quad (7d)$$

It is worth noting that this problem does not have any coupling constraint between one vehicle and another. Solving problem (7) or solving V independent optimization problems (one per vehicle) would lead to the same solution.

3.2 Coordinated charging

The charging process of all EVs is scheduled so that their charging demand does not determine violations of the grid constraints on nodal voltage magnitudes and line currents. The power flow at the substation transformer, also an important operational constraint, is not specifically considered here because it is never activated in the considered case study. Grid constraints are modelled in problem (7) with the linearized grid models discussed in Section 2. Quantities $\underline{v},\overline{v}$ denote the admissible voltage magnitude and $\overline{i}_l$ the line ampacity. The

problem formulation is:

$$\underset{P_{11}^{(\text{EV})},\dots,P_{TV}^{(\text{EV})}\in\mathbb{R}_+}{\arg\min}\left\{\sum_{t=1}^{T}\sum_{v=1}^{V}\left(\text{SOC}_{tv}-\text{SOC}_v^*\right)^2\right\} \quad (8a)$$

subject to:

SOC constraints (7b), (7c)	for all t and v	(8b)
$0\leq P_{tv}^{(\text{EV})}\leq\overline{S}_v^{(\text{EV})}$	for all t and v	(8c)
Nodal injections (1a), (1b), and (6)	for all t and n	(8d)
Linearized grid models (2)-(3)	for all t, n and l	(8e)
$\underline{v}\leq v_{tn}\leq\overline{v}$	for all t and n	(8f)
$i_{tl}\leq\overline{i}_l$	for all t and l	(8g)

Compared to (7), problem (8) features coupling constraints, given by the grid model, which requires the information on all nodal injections. This formulation requires gathering all the vehicles' information and the grid in a single (centralized) optimization problem. Centralized formulations of this kind can be used to derive signals to incentive or disincentivize the charge of EVs and achieve a form of indirect control (e.g., [9]).

3.3 Coordinated charging with reactive power support

We extend problem (8) by allowing chargers to inject/absorb reactive power with the the objective of controlling the voltage of the MV grid (where the reactance of the lines' longitudinal components may be dominant over the resistance and so reactive power control can be an effective way to provide voltage regulation). The vector of $2\times V\times T$ decision variables is denoted by:

$$\boldsymbol{x}=\left[P_{11}^{(\text{EV})},\dots,P_{TV}^{(\text{EV})},Q_{11}^{(\text{EV})},\dots,Q_{TV}^{(\text{EV})}\right]. \quad (9)$$

The decision-making problem for both EV chargers' active and reactive power is:

$$\underset{\boldsymbol{x}}{\arg\min}\left\{\sum_{t=1}^{T}\sum_{v=1}^{V}\left(\text{SOC}_{tv}\left(P_{tv}^{(\text{EV})}\right)-\text{SOC}_v^*\right)^2\right\} \quad (10a)$$

subject to

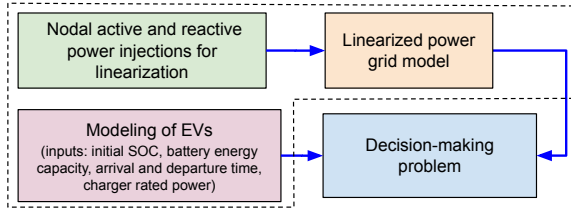|		
SOC constraints (7b), (7c)	for all t and v	(10b)
$\left(P_{tv}^{(\text{EV})}\right)^2+\left(Q_{tv}^{(\text{EV})}\right)^2\leq\left(\overline{S}_v^{(\text{EV})}\right)^2$	for all t and v	(10c)
$P_{tv}^{(\text{EV})}\geq 0$	for all t and v	(10d)
Nodal injections (1a), (1b), and (6)	for all t and n	(10e)
Linearized grid models (2)-(3)	for all t, n and l	(10f)
Grid constraints (8f)-(8g)	for all t, n and l	(10g)

Fig. 2. Workflow problem formulation using OPF.

4 Case study

We consider the European version of the CIGRE benchmark grid for MV systems from [5]. Its topology is shown in Fig. 1. The LV grids connected at the various nodes of the MV network are modeled in terms of their aggregated contributions. No violations of grid constraints are assumed in the LV grids. The MV grid is modelled with a single-phase equivalent assuming a balanced grid with transposed conductors. The nominal power, the power factor, and the number of parked EVs per node are reported in Table 1. Input information related to EVs are discussed in the next paragraph. The time-varying active power demand is modeled with the load coincidence factor model defined in [5]. The reactive power demand is modeled as the product between the active power and the tangent of arc-cosine of the power factor in Table 1. Line ampacities are chosen based on the conductor diameter. Statutory voltage levels are $1 \pm 3\%$. Computing sensitivity coefficients for the linear grid models requires nominal active and reactive nodal injections to compute the linearization, for which we use the nodal power injections of the net demand from the CIGRE specifications.

Table 1 Nodal nominal demand per node and number of EVs

Node	Apparent Power [kVA]	Power factor	Number of EVs
1	15'300	0.98	0
2	0	0	0
3	285	0.97	68
4	445	0.97	106
5	750	0.97	178
6	565	0.97	134
7	0	0	0
8	605	0.97	144
9	0	0	0
10	490	0.97	116
11	340	0.97	81
12	15'300	0.98	0
13	0	0	0
14	215	0.97	51

The numbers of EVs per node reported in Table 1 are estimated assuming approx. 1.4 EVs per household in average.*

---

*Except for nodes 1 and 12, which have no EVs to reduce the number of optimization variables. This approximation is deemed reasonable because these

The work in [10] considers 1.3 EVs per household in average, in-line with our estimate. The number of household per node is estimated as the ratio between the nominal power of each residential node and the contractual power of a household (6 kVA). In total for the whole grid (that, excluding nodes 2 and 12, refers to a total rated power of 30 MVA), we consider 878 EVs. The work in [11] considers 2'340 EVs for a 5 MVA MV residential grid, denoting that more intense loading situations due to EVs may exist. The SOC at arrival are sampled from statistical distributions estimated from data [12, 13]. The arrival time is assumed 16h for all vehicles. The energy capacity of the EV battery is 16 kWh for all EVs, also from [13]. The rated power of the chargers is 3.6 kVA, and their efficiency is 0.9 and power factor 1.

5 Results and Discussions

Three cases are considered:

- Case 1: uncoordinated charging (problem (7)),
- Case 2: grid-aware coordinated charging (problem (8)), and
- Case 3: coordinated charging with reactive power to support voltage regulation (problem (10)).

Fig. 3 shows the nodal voltage magnitudes in the three cases. Case 1 shows under-voltage conditions in evening hours. Under-voltages are due to evening peak power demand in combination with the start of the overnight charging process of the EVs. They appear at all nodes, except for those near the grid connection point. In Case 2, voltage levels at the voltage-critical nodes hit the lower bound at time 16:00 and remain there until 22:00, without, however, any under-voltage problems. This is thanks to enforcing in the decision-making problem the grid model and grid constraints. The line current constraints (not shown here for a reason of space) are respected. Case 3, features similar results as Case 2. This is to expect as both Case 2 and Case 3 implement grid constraints.

The average SOC level across the population of EVs is shown in 1. Case 1 achieves the fastest recharging time, at the price, however, of violating voltage constraints, as just discussed. This performance is to be expected because the charging power is bounded by the rated power of the chargers only, in (7d). Case 2 scores the slowest charging times. Case 3 improves the charging times of Case 2 thanks to using reactive power to improve the voltage levels, ultimately enabling more EVs to recharge.

Fig. 5 shows the results of a (linear) load flow for Case 3 where the contribution of reactive power is set to zero after that the optimization is solved. As visible, voltage constraints are violated, demonstrating that reactive power is here fundamental to improve voltage levels.

---

nodes are near upper grid's connection, so less critical for grid constraints violations.

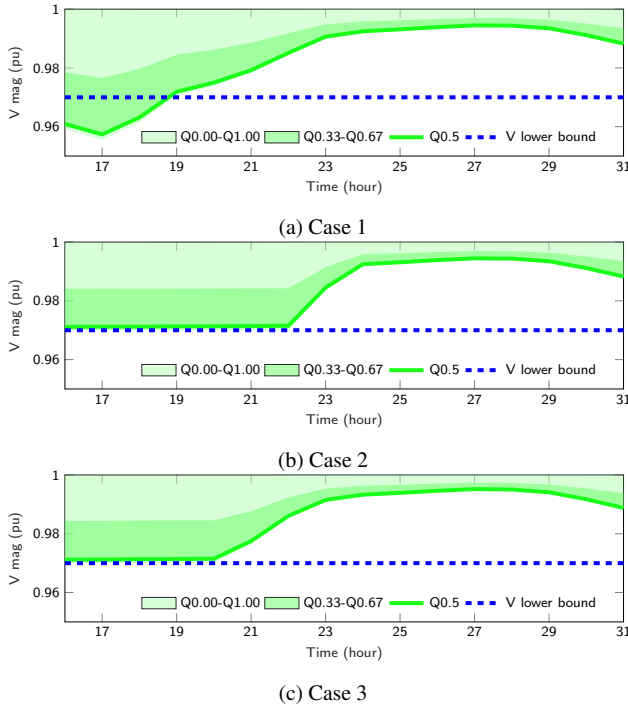(a) Case 1

(b) Case 2

(c) Case 3

Fig. 3 Nodal voltage magnitudes over the EVs charging horizon. The dashed lines are the voltage limits. The shaded bands denote different quantile intervals across the nodes.
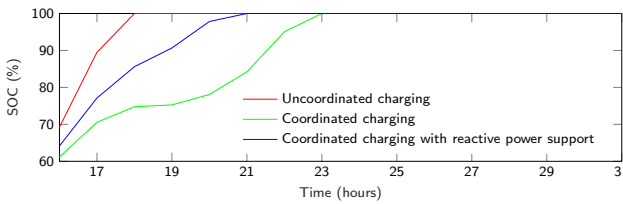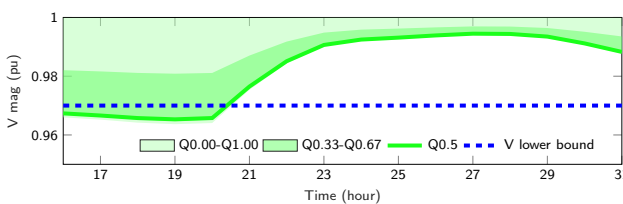

Fig. 4. Average SOC across the EVs population.

Fig. 5 Nodal voltage magnitudes in Case 3 after setting reactive power injections to zero.

6   Conclusions

This work investigated the problem of uncoordinated and coordinated charging of EVs in an MV grid, including reactive power support to improve voltage levels. It was shown that the uncoordinated charging of 878 EVs in the afternoon/evening period is conducive to violate the grid's voltage constraints. Grid-aware coordinated charging managed to solve the problem, at the price of deferring by a few hours the achievement of all vehicles' recharging objective. Using the spare capacity of the 2-quadrant controlled rectifiers of the chargers to provide reactive power contributed to improving the voltage levels, ultimately allowing more chargers to operate and shortening the overall charging times.

References

[1] "EU 2030 climate & energy framework," https://bit.ly/2P7PI0N, accessed: 2020-07.

[2] K. Knezovic, "Active integration of electric vehicles in the distribution network - theory, modelling and practice," Ph.D. dissertation, Technical University of Denmark (DTU), 2017.

[3] IRENA, "Innovation outlook: Smart charging for electric vehicles," International Renewable Energy Agency, Abu Dhabi, Tech. Rep. MSU-CSE-06-2, 2019.

[4] J. A. P. Lopes, F. J. Soares, and P. M. R. Almeida, "Integration of electric vehicles in the electric power system," *Proceedings of the IEEE*, vol. 99, no. 1, pp. 168–183, 2011.

[5] C. T. F. C6.04.02, "Benchmark systems for network integration of renewable and distributed energy resources," Cigre' International Council on large electric systems, Tech. Rep., July 2009.

[6] K. Christakou, J. LeBoudec, M. Paolone, and D. Tomozei, "Efficient computation of sensitivity coefficients of node voltages and line currents in unbalanced radial electrical distribution networks," *IEEE Transactions on Smart Grid*, vol. 4, no. 2, pp. 741–750, 2013.

[7] R. Gupta, F. Sossan, and M. Paolone, "Performance assessment of linearized opf-based distributed real-time predictive control," in *2019 IEEE Milan PowerTech*, 2019, pp. 1–6.

[8] F. Sossan, B. Mukherjee, and Z. Hu, "Impact of the charging demand of electric vehicles on distribution grids: a comparison between autonomous and non-autonomous driving," in *2020 Fifteenth International Conference on Ecological Vehicles and Renewable Energies (EVER)*, 2020, pp. 1–6.

[9] J. Hu, S. You, M. Lind, and J. Østergaard, "Coordinated charging of electric vehicles for congestion prevention in the distribution grid," *IEEE Transactions on Smart Grid*, vol. 5, no. 2, 2014.

[10] S. Johansson, J. Persson, S. Lazarou, and A. Theocharis, "Investigation of the impact of large-scale integration of electric vehicles for a swedish distribution network," *Energies*, vol. 12, no. 24, 2019. [Online]. Available: https://www.mdpi.com/1996-1073/12/24/4717

[11] N. Leemput, F. Geth, J. Van Roy, P. Olivella-Rosell, J. Driesen, and A. Sumper, "Mv and lv residential grid impact of combined slow and fast charging of electric vehicles," *Energies*, vol. 8, no. 3, 2015.

[12] P. B. Andersen, "Intelligent electric vehicle integration-domain interfaces and supporting informatics," Ph.D. dissertation, Technical University of Denmark (DTU), 2013.

[13] "Test-an-EV project: Electrical vehicle (ev) data," http://mclabprojects.di.uniroma1.it/smarthgnew/Test-an-EV/?EV-code=EV8, accessed: 2020-02.

5